A Precision Measurement of Electroweak Parameters in Neutrino-Nucleon Scattering

CCFR/NuTeV Collaboration
K. S. McFarland[3], C. G. Arroyo[2], B. J. King[2], L. de Barbaro[5], P. de Barbaro[7], A. O. Bazarko[2], R. H. Bernstein[3], A. Bodek[7], T. Bolton[4], H. Budd[7], L. Bugel[3], J. Conrad[2], R. B. Drucker[6], D. A. Harris[7], R. A. Johnson[1], J. H. Kim[2], T. Kinnel[8], M. J. Lamm[3], W. C. Lefmann[2], W. Marsh[3], C. McNulty[2], S. R. Mishra[2], D. Naples[4], P. Z. Quintas[2], A. Romosan[2], W. K. Sakumoto[7], H. Schellman[5], F. J. Sciulli[2], W. G. Seligman[2], M. H. Shaevitz[2], W. H. Smith[8], P. Spentzouris[2], E. G. Stern[2], M. Vakili[1], U. K. Yang[7], J. Yu[3], and G. P. Zeller[5]
University of Cincinnati, Cincinnati, OH 45221
Columbia University, New York, NY 10027
Fermi National Accelerator Laboratory, Batavia, IL 60510
Kansas State University, Manhattan, KS 66506
Northwestern University, Evanston, IL 60208
University of Oregon, Eugene, OR 97403
University of Rochester, Rochester, NY 14627
University of Wisconsin, Madison, WI 53706
(Received 20 March 1997)

Abstract

The CCFR collaboration reports a precise measurement of electroweak parameters derived from the ratio of neutral-current to charged-current cross-sections in neutrino-nucleon scattering at the Fermilab Tevatron. We determine $\sin^2\theta_W^{(\mathrm{on-shell})} = 0.2236 \pm 0.0028(\mathrm{expt.}) \pm 0.0030(\mathrm{model})$ for $m_{\mathrm{top}} = 175$ GeV, $m_{\mathrm{Higgs}} = 150$ GeV. This is equivalent to $M_W = 80.35 \pm 0.21$ GeV. The good agreement of this measurement with Standard Model expectations implies the exclusion of additional $\nu\nu qq$ contact interactions at 95% confidence at a mass scale of 1-8 TeV, depending on the form of the contact interaction.

In the early 1980's, accurate measurements of neutrino neutral-current scattering cross-sections provided key input to the Standard Model's predictions of the W and Z boson masses. Even with the production of copious on-shell W and Z bosons at high luminosity $p\overline{p}$ and e^+e^- colliders, neutrino-nucleon (νN) scattering still provides a measurement of electroweak parameters, in particular M_W/M_Z, with comparable precision. More importantly, the high precision comparison among these distinct electroweak processes differing in q^2 by more than two orders of magnitude provides a critical test of the theory and the possibility to search for non-Standard Model contributions with very high mass scales or low probabilities [1,2]. The measurement presented here represents the most precise determination of $\sin^2\theta_W$ from νN scattering to date and supersedes the previous result from CCFR [3] due to increased statistics and improved evaluation of systematic errors.

The neutral-current (NC) and charged-current (CC) νN deep inelastic scattering differential cross-sections on an isoscalar target of light quarks are related by

$$\begin{aligned}\frac{d}{dxdq^2}\left(\sigma_{\mathrm{NC}}^{\nu,\overline{\nu}}\right) &= \left(u_L^2+d_L^2\right)\frac{d}{dxdq^2}\left(\sigma_{\mathrm{CC}}^{\nu,\overline{\nu}}\right)\\ &\quad+\left(u_R^2+d_R^2\right)\frac{d}{dxdq^2}\left(\sigma_{\mathrm{CC}}^{\overline{\nu},\nu}\right)\end{aligned} \tag{1}$$

where $u_{L,R}$ and $d_{L,R}$ are the left(L) and right(R)-handed couplings of the Z^0 to up and down quarks, respectively. Small corrections to Eqn. 1 arise from massive quark production suppression, CKM matrix effects, higher-twist processes, electromagnetic and electroweak radiative corrections, and from any isovector component in the target, including heavy quark seas. Within the Standard Model, these left and right-handed couplings are given by $I^{(3)}_{\mathrm{Weak}}-Q_{\mathrm{EM}}\sin^2\theta_W$ and $-Q_{\mathrm{EM}}\sin^2\theta_W$, respectively, allowing a measurement of $\sin^2\theta_W$ from ratios of NC to CC, and ν to $\overline{\nu}$ CC cross-sections. Furthermore, if the expression for $\sigma^{\nu}_{\mathrm{NC}}$ in Eqn. 1 is used to extract $\sin^2\theta_W$, it is almost equal to $\sin^2\theta_W$ in the "on-shell" renormalization scheme ($\sin^2\theta_W^{(\mathrm{on-shell})}\equiv 1-M_W^2/M_Z^2$ to all orders), independent of m_{top} and m_{Higgs} [4,5]. Therefore, the measurement of $\sin^2\theta_W$ from νN scattering, combined with the precise measurements of M_Z from LEP [6], implies a measurement of M_W. In addition, direct extraction of $u_{L,R}$ and $d_{L,R}$ also allows a search for a variety of non-Standard Model processes through comparison of the measurements from νN scattering with Standard Model expectations.

The CCFR detector consists of an 18 m long, 690 ton neutrino target calorimeter with a mean density of 4.2 g/cm^3, followed by an iron toroid spectrometer. The target calorimeter consists of 168 iron plates, 3m $\times$ 3m $\times$ 5.1cm apiece. The active elements are liquid scintillation counters spaced every two plates (10.2 cm of steel) and drift chambers spaced every four plates (20.4 cm of steel). There are a total of 84 scintillation counters and 42 drift chambers in the target. The neutrino target is approximately isoscalar, with a 5.67% neutron excess. The toroid spectrometer is not directly used in this analysis.

The Fermilab Tevatron Quadrupole Triplet neutrino beam is created by decays of pions and kaons produced when 800 GeV protons hit a BeO target. A wide band of secondary energies is accepted by downstream focusing magnets. The target is located about 1.4 km upstream of the neutrino detector. The target and focusing train are followed by a 0.5 km decay region. The interactions of the beam are predominantly from muon neutrinos (86%) and anti-neutrinos (12%), but also include a small fraction of electron neutrinos (2.3%). The mean energies of the ν_μ, $\overline{\nu}_\mu$, and $\nu_e(\overline{\nu}_e)$ events are 165, 135 and 160 GeV, respectively. The mean q^2 exchanged in the neutrino interactions used in this analysis was -35 GeV^2.

Neutrinos are observed *via* their NC and CC interactions, both of which are selected in this analysis from the energy transferred to the struck quark which appears as a hadronic shower in the target calorimeter. The hadronic energy is measured by the variable E_{cal},

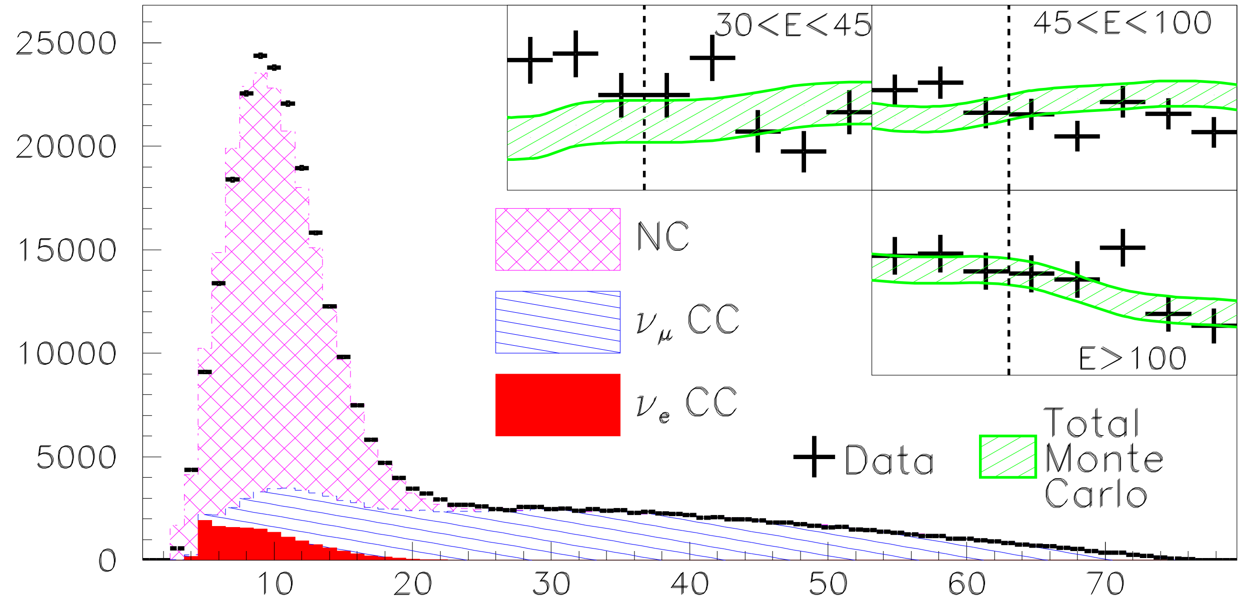

FIG. 1. Event length in data and Monte Carlo. The prediction for NC, CC $\nu_\mu(\overline{\nu}_\mu)$, and CC $\nu_e(\overline{\nu}_e)$ interactions is shown. Inset are comparisons in the region of the length cut of data and Monte Carlo with systematic errors shown.

which is the sum of energies observed in the first 20 scintillation counters (2.1m equivalent of steel) in the target downstream of the interaction vertex. NC events usually have no final-state muon and deposit energy over a range of counters typical of a hadronic shower (5 to 20 counters). ν_μ CC events are distinguished by the presence of a muon in the final state which deposits energy typical of a minimum ionizing particle in a large number of consecutive scintillation counters downstream of the hadronic shower.

A "length" is defined for each event as the number of counters between the interaction vertex and the last counter consistent with the energy deposition expected from a single muon passing through the calorimeter. Events with a "short" length are identified as NC candidates. The separation between short and "long" events is made at 20 counters (2.1m of steel) for events with $E_{\rm cal} \leq 45$ GeV, 25 counters (2.6m of steel) for events with $45 < E_{\rm cal} \leq 100$ GeV, and 30 counters (3.1m of steel) for events with $E_{\rm cal} > 100$ GeV. As is shown in the length distributions in Figure 1, NC interactions lie in a clear peak, well-below the length cut, with a continuous band of CC ν_μ interactions under the peak. The CC ν_μ background is calculated to be 10.5%, 21.3%, and 21.2% of the "short" NC candidates in the three $E_{\rm cal}$ regions, respectively.

The data used in this analysis were taken between 1984 and 1988 in FNAL experiments E-744 and E-770. Events were required to have $E_{\rm cal} > 20$ GeV to ensure full efficiency of the trigger [3]. Fiducial cuts were made on the location of the neutrino interaction in the calorimeter to ensure that events were neutrino-induced, that a separation between long and short events could be made, and that events originated in the central part of the calorimeter to maximize containment of wide-angle muons and to minimize the ratio of electron to muon neutrinos. The resulting data sample consisted of 8.1×10^5 events, and from these events the ratio

$$R_{\text{meas}} = \frac{\#\text{ of short events}}{\#\text{ of long events}} = 0.4151 \pm 0.0010$$

was calculated.

A detailed Monte Carlo was used to determine electroweak parameters from R_{meas}. The only undetermined inputs to this Monte Carlo were the neutral current quark couplings which were then varied until the Monte Carlo predicted an R_{meas} which agreed with that observed in the data. For the extraction of $\sin^2\theta_W$, the couplings in the Monte Carlo were fixed to their Standard Model predictions as functions of $\sin^2\theta_W$, which was then varied as the only free parameter. The Monte Carlo included detector response and beam simulations, as well as a detailed cross-section model which included electromagnetic radiative corrections, isovector target corrections, heavy quark production and seas, the longitudinal cross-section, and lepton mass effects.

There are three major uncertainties in the comparison of R_{meas} from the Monte Carlo to the data: the statistical error in the data, the uncertainty in the effective charm quark mass for charged current charm production, and the uncertainty in the incident flux of ν_e's on the detector.

The charm quark mass error comes from the uncertainty in modeling the mass threshold of the charm production cross section. The Monte Carlo uses a slow-rescaling model with the parameters extracted using events with two oppositely charged muons (e.g., $\nu q \to \mu^- c$, $c \to \mu^+ X$) from this experiment [7]. The shape and magnitude of the strange sea were also extracted in the same analysis and were used in the Monte Carlo cross-section model. This error dominates the calculation of R_{meas} at low E_ν (and low E_{cal}) where the threshold suppression is greatest.

The $\nu_e(\overline{\nu}_e)$ flux uncertainty has an important effect on R_{meas} because almost all charged current $\nu_e(\overline{\nu}_e)$ events are short events. Therefore, the relatively small fractional uncertainty in the $\nu_e(\overline{\nu}_e)$ flux is a significant effect, particularly at high E_{cal} since most $\nu_e(\overline{\nu}_e)$ charged current interactions deposit the full incident neutrino energy into the calorimeter. Two techniques were used to determine the $\nu_e(\overline{\nu}_e)$ flux. In both E744 and E770, a detailed beam Monte Carlo was used to predict the flux, up to a 4.1% uncertainty in each experiment. This 4.1% is dominated by a 20% production uncertainty in the K_L content of the secondary beam which produces 16% of the ν_e flux. The bulk of the ν_e flux comes from $K^{\pm}_{e3}$ decays, which are well-constrained by the observed ν_μ spectrum from $K^{\pm}_{\mu 2}$ decays [3]. In E770, the $\nu_e(\overline{\nu}_e)$ flux was measured directly using the fact that CC $\nu_e(\overline{\nu}_e)$ interactions will have a high fraction of their energy deposited in the first three counters downstream of the event vertex. This gave an independent measurement of the $\nu_e(\overline{\nu}_e)$ flux with a uncertainty of 3.5% which was in good agreement with the Monte Carlo method [8]. Combining these techniques, a measurement of the $\nu_e(\overline{\nu}_e)$ flux sum in E744 and E770 is obtained with a 2.9% error.

Other sources of experimental uncertainties were kept small through extensive modeling based on neutrino and testbeam data [9–11]. The cross-section model used a modified Buras-Gaemers parameterization [12] of the CCFR data for input parton distributions. This resulted in partial cancellations of certain systematic effects, such as errors in energy calibration. Systematic uncertainties associated with the measurement of E_{cal} include possible small NC/CC shower differences (constrained by a LEPTO Monte Carlo study [3]), uncertainties in the muon energy deposit within the hadron shower, uncertainties in the resolu-

SOURCE OF UNCERTAINTY	$\delta \sin^2 \theta_W$
data statistics	0.0019
Monte Carlo statistics	0.0004
TOTAL STATISTICS	0.0019
ν_e flux	0.0015
Transverse Vertex	0.0004
Energy Measurement	
Hadron Energy Scale (1%)	0.0004
Muon Energy Loss in Shower	0.0003
Muon Energy Scale (1%)	0.0002
Event Length	
Hadron Shower Length	0.0007
Counter Efficiency and Noise	0.0006
Vertex Determination	0.0003
TOTAL EXP. SYST.	0.0019
Charm Production, $\overline{s}$	
($m_c = 1.31 \pm 0.24$ GeV)	0.0027
Higher Twist	0.0010
Longitudinal Cross-Section	0.0008
Charm Sea, ($\pm 100\%$)	0.0006
Non-Isoscalar Target	0.0004
Structure Functions	0.0002
Rad. Corrections	0.0001
TOTAL PHYSICS MODEL	0.0030
TOTAL UNCERTAINTY	0.0041

TABLE I. Uncertainties in the extraction of $\sin^2 \theta_W^{(\mathrm{on-shell})}$ from the CCFR data

tion function, e/π response, and absolute energy scales obtained from hadron and electron test beam measurements [9,10]. The length uncertainties include those associated with the shower length parameterizations of test beam measurements [11], the calorimeter longitudinal vertex determination (studied using the vertex from events with two muon tracks), counter inefficiencies and noise, and counter spatial dimensions. In the cross-section model, the level of the charm sea was taken from the CTEQ4L parton distribution functions and was assigned a 100% uncertainty. Our parameterization of $R_{\mathrm{long}} = \sigma_L/\sigma_T$ is based on QCD predictions and data from charged lepton scattering experiments [13] and is varied by 15% of itself to estimate uncertainties. A correction for the difference between u and d valence quark distributions in nucleons, obtained from muon scattering data [14], was applied to account for the 5.67% excess of neutrons over protons in the target. A correction was also applied for the asymmetry in the u and d sea distributions suggested by the NA51 Drell-Yan data [15] and the Gottfried Sum Rule as measured in muon scattering [16]. Radiative corrections to the scattering cross-sections were applied using computer code supplied by Bardin [17] and 1-loop electroweak radiative corrections as calculated by Marciano and Sirlin

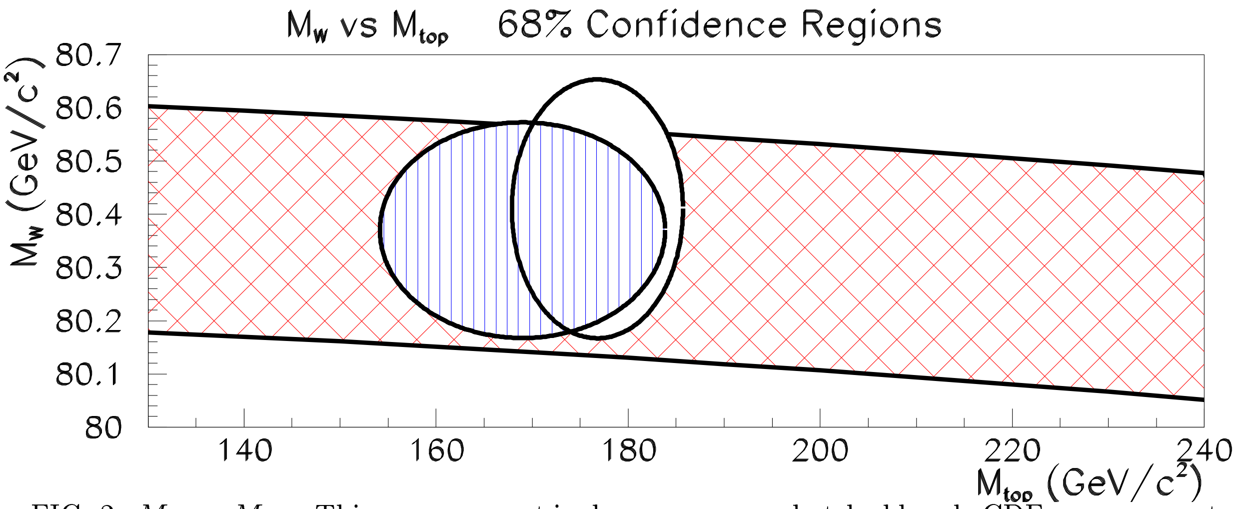

FIG. 2. M_W vs $M_{\rm top}$. This measurement is shown as a cross-hatched band. CDF measurements provide the hollow ellipse, and the D0 measurements are shown in the striped ellipse.

[4]. Possible higher-twist corrections were parameterized in a VDM-based model of Pumplin [18] which was constrained by lepto-production data. Table I shows the uncertainties in the determination of $\sin^2\theta_W$.

The extraction of $\sin^2\theta_W^{\rm (on-shell)}$ by comparing $R_{\rm meas}$ in the data to the Monte Carlo with $\sin^2\theta_W^{\rm (on-shell)}$ as the single free parameter yields,

$$\begin{aligned}\sin^2\theta_W^{\rm (on-shell)} &= 0.2236 \pm 0.0028((\text{expt.}) \pm 0.0030(\text{model}) \\ &\quad +0.0006 \times \left(\frac{(m_{\rm top}^2 - (175\ \text{GeV})^2)}{(100\ \text{GeV})^2}\right) \\ &\quad -0.0002 \times \log_e\left(\frac{m_{\rm Higgs}}{150\ \text{GeV}}\right). \end{aligned} \tag{2}$$

The explicit dependence of the central value of this result on m_c is $0.2236 + 0.0111 \times (m_c - 1.31\ \text{GeV})$. Only data with $E_{\rm cal} > 30$ GeV was used in this result to reduce the effect of the charm-production and higher-twist systematics which are largest at low $E_{\rm cal}$. Since $\sin^2\theta_W^{\rm (on-shell)} \equiv 1 - M_W^2/M_Z^2$, this result implies $M_W = 80.35 \pm 0.21$ GeV. This value of M_W agrees with direct mass measurements [19] as shown in Figure 2, and this result is also in good agreement both with previous νN measurements and with Standard Model expectations [6].

$R_{\rm meas}$ is also used to extract a constraint on the couplings of quarks to the Z^0:

$$\begin{aligned}\kappa = 0.5820 \pm 0.0041 &= 1.7897 g_L^2 + 1.1479 g_R^2 \\ &\quad -0.0916\delta_L^2 - 0.0782\delta_R^2,\end{aligned} \tag{3}$$

where $g_{L,R}^2 = u_{L,R}^2 + d_{L,R}^2$ and $\delta_{L,R}^2 = u_{L,R}^2 - d_{L,R}^2$. The explicit dependence of the central value of κ on m_c is $\kappa = 0.5820 - (m_c - 1.31) * 0.0111$. The Standard Model prediction is $\kappa = 0.5817 \pm 0.0013$ for the measured values of m_Z, $m_{\rm top}$, m_W. Figure 3 compares this result to other neutrino data [20] and the Standard Model prediction [6].

Because the CCFR result for neutral-current quark couplings are in good agreement with Standard Model expectations, this result disfavors the introduction of additional processes

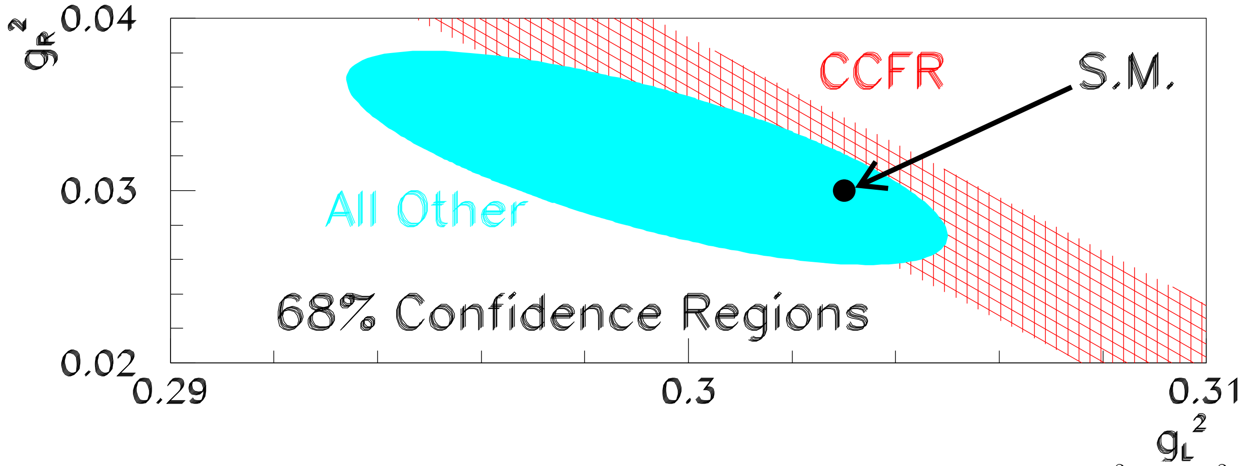

FIG. 3. One-sigma constraints on the isoscalar neutral current quark couplings, g_L^2 and g_R^2, from this result (hatched) and from other neutrino data (solid).

Interaction	Λ^+	Λ^-
Neutrino Interactions Only		
LL	4.6 TeV	5.1 TeV
LR	4.1 TeV	4.3 TeV
LV	6.5 TeV	6.5 TeV
LA	2.1 TeV	3.2 TeV
Antineutrino Interactions Only		
LL	1.3 TeV	2.2 TeV
LR	3.8 TeV	4.0 TeV
LV	4.3 TeV	4.5 TeV
LA	3.1 TeV	3.7 TeV
Neutrino and Anti-Neutrino		
LL	5.0 TeV	5.4 TeV
LR	5.8 TeV	5.8 TeV
LV	7.9 TeV	7.8 TeV
LA	3.0 TeV	1.8 TeV

TABLE II. 95% Confidence Lower Limits on mass scales of new $\nu\nu qq$ contact terms from CCFR.

contributing to the same final state. To quantify this, we use the CCFR data to constrain models of new $\nu\nu qq$ contact interactions. Such models are often used to parameterize searches for fermion compositeness or non-zero size [21]. We assume a generation-universal interaction of the form

$$-\mathcal{L} = \sum_{H_q \in \{L,R\}} \frac{\pm 4\pi}{\left(\Lambda^{\pm}_{LH_q}\right)^2} \times \left\{ \overline{l_L}\gamma^\mu l_L \overline{q_{H_q}}\gamma_\mu q_{H_q} + l_L\gamma^\mu \overline{l_L}\,\overline{q_{H_q}}\gamma_\mu q_{H_q} + \overline{l_L}\gamma^\mu l_L q_{H_q}\gamma_\mu \overline{q_{H_q}} + l_L\gamma^\mu \overline{l_L} q_{H_q}\gamma_\mu \overline{q_{H_q}} \right\}. \tag{4}$$

Such interactions would shift one or more of the quark couplings in ν or $\overline{\nu}$ induced interactions from its Standard Model value [1]. Only limits for couplings to left-handed neutrinos (and right-handed couplings to anti-neutrinos) are given, since the charged-current weak interactions which produce the neutrinos in the beamline are assumed to have only Standard Model contributions. One-sided 95% confidence level lower limits for each Λ are set by finding the points in the space of measured couplings at which the χ^2 is 1.64 units above the minimum, and then determining the Λ to which these points correspond in each model [1]. Limits for LL, LR, LV (vector, $\Lambda_{LL} = \Lambda_{LR}$) and LA (axial-vector, $\Lambda_{LL} = -\Lambda_{LR}$) are shown in Table II. Limits are shown for the cases when this new contact term affects neutrinos interactions only, when it affects anti-neutrino interactions only, and when it affects both neutrino and anti-neutrino interactions. These limits are roughly comparable to the limits for charged lepton-quark interactions in $p\overline{p}$ collider data from the Fermilab Tevatron [22].

In summary, CCFR has produced the most precise measurements of neutral-current neutrino-nucleon interactions to date, and has used these measurements to constrain neutral-current coupling to quarks. Within the Standard Model, this leads to a measurement of $\sin^2\theta_W^{(\mathrm{on-shell})} = 0.2236 \pm 0.0041$ ($m_{\mathrm{top}} = 175$ GeV, $m_{\mathrm{Higgs}} = 150$ GeV) which corresponds to $M_W = 80.35 \pm 0.21$ GeV. This result is also used to limit possible TeV-scale contact interactions of neutrinos and quarks outside the Standard Model.

This research was supported by the U.S. Department of Energy and the National Science Foundation. We thank the staff of the Fermi National Accelerator Laboratory for their hard work in support of this experimental effort. We also wish to thank Bill Marciano for helpful suggestions regarding the presentation of the limits on new contact interactions.

[1] In the case of many of these computations, there are actually two solutions for such a Λ, one at comparatively high energy, and one at low energy where a cancellation among large changes in the individual quark chiral couplings results in no change in the measured quantity, κ, defined in Eqn. 3. In each one of these cases, the changes in one or more of the individual couplings are so large that the possibility of such an interaction is already excluded by less precise data on individual quark chiral couplings [20]. Therefore, only the high-mass lower limits on Λ given by the procedure in the text are reported here.

REFERENCES

[1] P. Langacker *et al.*, Rev. Mod. Phys. **64**, 87 (1991).

[2] K.S. McFarland, D. Naples *et al.*, Phys. Rev. Lett., **75**, 3993 (1995).

[3] C. Arroyo, B.J. King *et al.*, Phys. Rev. Lett., **72**, 3452 (1994). See also B.J. King (NEVIS Report 284) and C. Arroyo (NEVIS Report 293), Ph.D. Theses, Columbia University.

[4] W.J. Marciano and A. Sirlin, Phys. Rev. **D22**, 2695 (1980).

[5] R.G. Stuart, Z. Phys. **C34**, 445 (1987).

[6] Particle Data Group, Phys. Rev. **D54**, 85 (1996).

[7] S.A. Rabinowitz *et al.*, Phys. Rev. Lett. **70**, 134 (1993).

[8] A. Romosan *et al.*, NEVIS-1529, submitted to Phys. Rev. Lett (1996).

[9] W.K. Sakumoto *et al.*, Nucl. Inst. Meth. **A294**, 179 (1990).

[10] B.J. King *et al.*, Nucl. Inst. Meth. **A302**, 254 (1990).

[11] F.S Merritt *et al.*, Nucl. Inst. Meth. **A245**, 27 (1986); P.H. Sandler *et al.*, Phys. Rev. **D42**, 759 (1990).

[12] A.J. Buras and K.J.F. Gaemers, Nucl. Phys. **B132**, 249 (1978).

[13] L.W. Whitlow. SLAC-Report-357, p.109 (1990).

[14] P. Amaudruz *et al.*, Nucl. Phys. **B371**, 3 (1992).

[15] A. Baldit *et al.*, Phys. Lett. **B332** 244 (1994).

[16] M. Arneodo *et al.*, Phys. Rev. **D50** 1 (1994).

[17] D. Yu. Bardin and O.M. Fedorenko, Sov. J. Nucl. Phys **30**, 418 (1979); and private communication.

[18] J. Pumplin, Phys. Rev. Lett. **64** 2751 (1990). $S_0 \leq 2$ GeV^2 is allowed by data summarized in M. Virchaux and A. Milsztajn, Phys. Lett. **B274**, 221 (1992).

[19] F. Abe *et al.*, Phys. Rev. **D52** 4784 (1995); J. Lys for the CDF collaboration, proceedings of ICHEP 1996, FERMILAB-CONF-96-409-E; M. Rijssenbeek for the D0 collaboration, proceedings of ICHEP 1996, FERMILAB-CONF-96/365-E; S. Protopopescu for the D0 collaboration, proceedings of ICHEP 1996.

[20] G. Fogli, D. Haidt, Z. Phys. **C40**, 379 (1988).

[21] E. Eichten, K. Lane and M. Peskin, Phys. Rev. Lett. **50**, 811 (1983).

[22] A. Bodek for the CDF collaboration, proceedings of ICHEP 1996, University of Rochester Preprint, UR-1482 (ER/40685/894); CDF-3870.